Knockouts of TUT7 and 3′hExo show that they cooperate in histone mRNA maintenance and degradation

CHRIS E. HOLMQUIST,[1,2,5] WENXIA HE,[2,3,5] RITA M. MEGANCK,[2,4] and WILLIAM F. MARZLUFF[2,3]

[1]Division of Medicinal Chemistry and Chemical Biology, University of North Carolina, Chapel Hill, North Carolina 27599, USA
[2]Integrated Program for Biological and Genome Sciences, University of North Carolina, Chapel Hill, North Carolina 27599, USA
[3]Department of Biochemistry and Biophysics, University of North Carolina, Chapel Hill, North Carolina 27599, USA
[4]Curriculum in Genetics and Molecular Biology, University of North Carolina, Chapel Hill, North Carolina 27599, USA

ABSTRACT

Metazoan histone mRNAs are the only cellular eukaryotic mRNAs that are not polyadenylated, ending instead in a conserved stem–loop. SLBP is bound to the 3′ end of histone mRNAs and is required for translation of histone mRNA. The expression of histone mRNAs is tightly cell-cycle regulated. A major regulatory step is rapid degradation of histone mRNA at the end of S-phase or when DNA synthesis is inhibited in S-phase. 3′hExo, a 3′ to 5′ exonuclease, binds to the SLBP/SL complex and trims histone mRNA to 3 nt after the stem–loop. Together with a terminal uridyl transferase, 3′hExo maintains the length of the histone mRNA during S-phase. 3′hExo is essential for initiating histone mRNA degradation on polyribosomes, initiating degradation into the 3′ side of the stem–loop. There is extensive uridylation of degradation intermediates in the 3′ side of the stem when histone mRNA is degraded. Here, we knocked out TUT7 and 3′hExo and we show that both modification of histone mRNA during S-phase and degradation of histone mRNA involve the interaction of 3′hExo, and a specific TUTase, TENT3B (TUT7, ZCCHC6). Knockout of 3′hExo prevents the initiation of 3′ to 5′ degradation, stabilizing histone mRNA, whereas knockout of TUT7 prevents uridylation of the mRNA degradation intermediates, slowing the rate of degradation. In synchronized 3′hExo KO cells, histone mRNA degradation is delayed, but the histone mRNA is degraded prior to mitosis by a different pathway.

Keywords: TUT7; cell cycle; histone mRNA; mRNA degradation; uridylation

INTRODUCTION

Replication-dependent histone mRNA levels are tightly regulated during the mammalian cell cycle, with histone mRNA accumulating at the beginning of S-phase and being rapidly degraded at the end of S-phase. The bulk of this regulation is post-transcriptional, and is mediated through the novel 3′ end of histone mRNA (Harris et al. 1991). Metazoan replication-dependent histone mRNAs are the only known cellular eukaryotic mRNAs that are not polyadenylated, ending instead in a conserved stem–loop rather than a poly(A) tail (Marzluff et al. 2008). Rapid degradation of the histone mRNA requires the stem–loop at the 3′ end of the mRNA, and translation of the histone mRNA (Graves et al. 1987; Pandey and Marzluff 1987; Kaygun and Marzluff 2005b). Several years ago, we reported that histone mRNAs were uridylated in the stem–loop when degradation was activated, either by inhibiting DNA replication or at the end of S-phase (Mullen and Marzluff 2008). Subsequently we developed a sequencing pipeline for efficient detection of nontemplated nucleotides on histone mRNAs and found that histone mRNAs were also uridylated at the 3′ end during S-phase (Welch et al. 2015; Lackey et al. 2016).

Processing of histone mRNA in the nucleus leaves a 5 nt tail after the stem–loop. 3′hExo (ERI1), which forms a ternary complex with the SL and SLBP at the 3′ end of histone mRNA (Yang et al. 2006; Tan et al. 2013), trims the histone mRNA, removing 2 nt from the 5 nt extension (Yang et al. 2006). If more than 2 nt is removed, a TUTase adds uridines to the 3′ end to restore the length of the tail to 3 nt during S-phase. Cells from knockout mice lacking 3′hExo did not rapidly degrade histone mRNA, implicating 3′hExo in the initial steps of histone mRNA degradation (Hoefig et al. 2013). 3′hExo initiates 3′ to 5′ degradation of histone mRNA on polyribosomes, with many of the degradation intermediates

[5]These authors contributed equally to this work.
Corresponding author: Marzluff@med.unc.edu
Article is online at http://www.rnajournal.org/cgi/doi/10.1261/rna.079233.122. Freely available online through the *RNA* Open Access option.

in the stem–loop being extensively uridylated (Slevin et al. 2014).

There are several terminal uridyl transferases, TUTases, which are members of a family of proteins that contain a noncanonical poly(A) polymerase domain (PAPD), which also include cytoplasmic poly(A) polymerases and poly(A) polymerases of the TRAMP complex. This family of proteins has been recently renamed as the TENT family of proteins (Warkocki et al. 2018). There are two major cytoplasmic uridyl transferases; TENT3A (TUT4 or ZCCHC11); and TENT 3B (TUT7 or ZCCHC6). These are large (>1400 aa) proteins with a common domain structure (Faehnle et al. 2017; Warkocki et al. 2018). For the uridylation of pre-miRNAs (Kim et al. 2015; Faehnle et al. 2017), miRNAs (Thornton et al. 2014), damaged structural RNAs (Thomas et al. 2015; Labno et al. 2016; Pirouz et al. 2016), and most polyadenylated mRNAs (Lim et al. 2014; Chang et al. 2018), either TENT3A or TENT3B can function in vivo.

TUT7 has been implicated in histone mRNA uridylation using RNA interference (Lackey et al. 2016). Here, we report the effect of knockout of TUT7 and 3′hExo in HCT116 cells on histone mRNA metabolism. We find that TUT7 is the primary uridyl transferase that modifies histone mRNA during S-phase to maintain the 3 nt tail, and that it exclusively functions to add the long U-tails on the 3′ side of the stem during initiation of histone mRNA degradation. Knockout of 3′hExo resulted in stabilization of histone mRNA, and more extensive uridylation of the 3′ end of histone mRNA. Similar effects were seen in synchronous S-phase cells treated with DNA synthesis inhibitors and cells exiting S-phase. Although 3′hExo KO stabilized histone mRNAs when DNA synthesis was inhibited, histone mRNAs were still degraded before mitosis in synchronized cells, suggesting there must be a second pathway to ensure histone mRNA degradation prior to mitosis.

RESULTS

TUT7 and 3′hExo KO cells are viable

To assess the role of TUT7 and 3′hExo in regulation of histone mRNA, we generated CRISPR-Cas9 stable knockout mutants of each gene in HCT116 colon carcinoma cells. HCT116 cells are roughly diploid (Brattain et al. 1983), which limits the number of alleles to target. Guide RNAs targeting the second exon of each gene were designed so they would disrupt the coding region early in the gene and avoid possible alternative translation start sites (Fig. 1A,B). Two TUT7 knockout lines and multiple (>6) lines of 3′hExo were obtained.

We subcloned the PCR products of the targeted regions and sequenced them to identify the changes that occurred in each allele. We analyzed two knockout lines for each gene in depth. The sequences of the disrupted alleles are shown in Figure 1B. We confirmed the knockout of the targeted proteins by western blotting (Fig. 1C,D). Note that we detect 2–3 species ([*] in Fig. 1C) with the TUT7 antibody, which is made against the amino-terminal region of the protein, and none of them are present in the KO cell lines. Whether these represent proteolytic cleavage products or alternatively spliced products is not known. We tested whether knockout of 3′hExo affected the expression of TUT7, and whether knockout of TUT7 affected the expression of 3′hExo or TUT4, a homolog of TUT7. Knockout of TUT7 resulted in approximately fourfold increased expression of TUT4 protein in both knockout cell lines (Fig. 1E; also see Fig. 5C), suggesting that the increase in TUT4 might compensate for an essential function of TUT7 for cell growth. Neither the levels of TUT7 or 3′hExo were changed by knockout of the other protein (Fig. 1F). Note that TUT4 and TUT7 are very similar proteins, and in most studies they have been found to participate in uridylating the same targets, including let7 pre-miRNA (Thornton et al. 2012; Faehnle et al. 2017); defective structural RNAs (Labno et al. 2016); maternal mRNAs (Morgan et al. 2017; Chang et al. 2018; Morgan et al. 2019); the oligo(A) tail remaining on deadenylated mRNAs (Lim et al. 2014); and mRNAs during apoptosis (Thomas et al. 2015).

Both TUT7 and 3′hExo KOs affect the 3′ termini of histone mRNA

To assay the effect of the knockout of TUT7 or 3′hExo on histone mRNA metabolism, we synchronized cells at the beginning of S-phase using a double thymidine block. After releasing the cells into S-phase for 3 h, we prepared RNA from the cells and confirmed they were in S-phase using flow cytometry combined with EdU labeling. We then prepared EnD-seq libraries as previously described, to determine the 3′ ends of the histone mRNAs, including identifying any nontemplated nucleotides (Slevin et al. 2014; Welch et al. 2015; Holmquist and Marzluff 2018). We sequenced the histone mRNAs to determine the 3′ termini of the mRNAs and degradation intermediates with single nucleotide resolution (Fig. 2). We show the results for two histone mRNAs, HIST2H2AA3 (H2AC18) and HIST1H2BF (H2BC7), and similar results were obtained for other histone mRNAs. (Note that the histone gene nomenclature is in the process of being changed [Seal et al. 2022]; the new names are H2AC18 and H2BC7.) Histone pre-mRNA is cleaved 5 nt after the stem–loop in the nucleus. The 3′ end of the histone mRNA in the cytoplasm has 2 nt trimmed off by 3′hExo (Mullen and Marzluff 2008). 3′hExo forms a complex on the 3′ end of the mRNA together with SLBP (Yang et al. 2006; Tan et al. 2013). If the 3′hExo removes one or two additional nucleotides in wild-type cells, a TUTase adds nontemplated uridines to replace them, restoring the mRNA length to 3 nt after the stem–loop (Welch et al. 2015; Lackey et al. 2016). The data are displayed by indicating the position of the last templated nt ("the index"), with

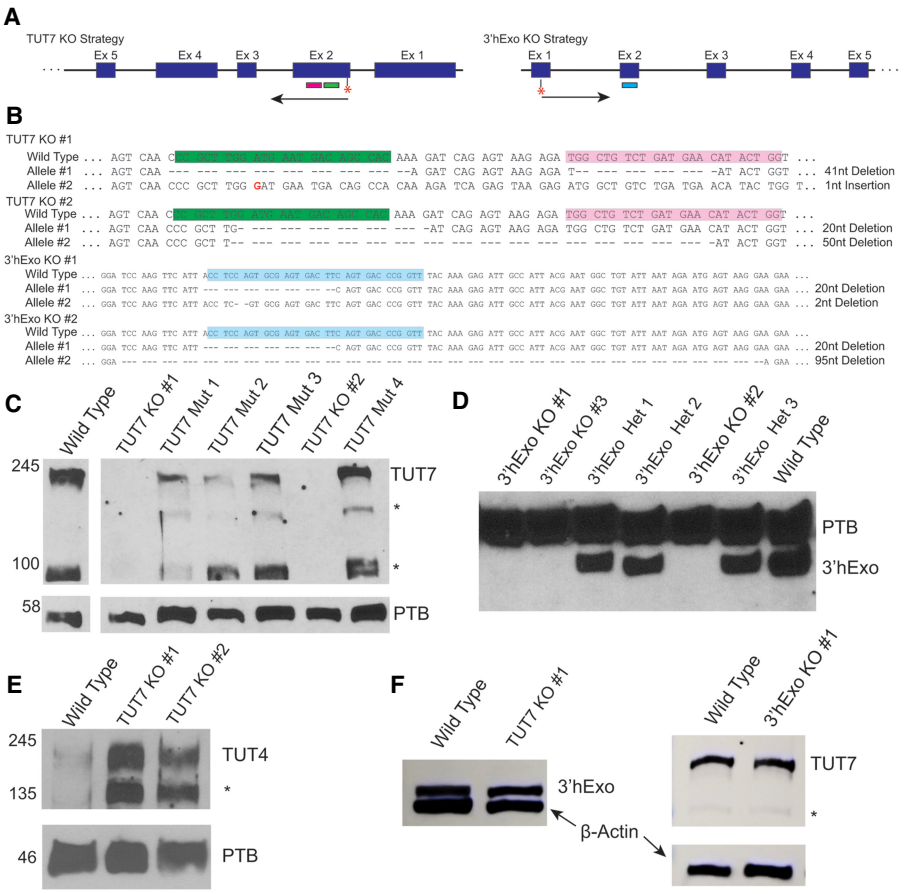

FIGURE 1. Characterization of 3′hExo and TUT7 KOs. (*A*) Structure of the *TUT7* (*left*) and *3′hExo* genes (*right*). The (*) indicates the start codon, and the colored boxes the location of the guide RNAs. (*B*) CRISPR strategy and results. The guide RNAs and NGG sequence are boxed. The two alleles for each KO were sequenced. Two independent TUT7 KO lines were isolated and several 3′hExo KO lines were isolated and two were characterized in detail. (*C*) Western blot analysis of potential TUT7 KOs. Six potential TUT7 KO lines were analyzed by western blotting. Four lines had only one allele inactivated and two had both alleles inactivated. (*D*) Western analysis of 3′hExo KOs. Three had both alleles inactivated and three were heterozygous, with a single allele inactivated. (*E*) The levels of TUT4 in the TUT7 KO cells were determined by western blotting. Each TUT7 KO had a substantial increase in expression of TUT4. (*F*) The levels of TUT7 and 3′hExo were determined in the KO of the other protein. The levels of TUT7 were similar to wild-type in the 3′hExo KO (*right*), and the levels of 3′hExo were similar to wild-type in the TUT7 KO (*left*). PTB or β-actin were analyzed as the loading control.

different colors indicating the addition of 0, 1, 2, or >2 nt at that position. After trimming of the 3′ end by 3′hExo, unmodified histone mRNAs end in ACC after the stem–loop (Fig. 2A, index 2). However, if one or two additional nucleotides are removed, then one or two uridines are added, restoring the tail to 3 nt after the stem–loop (Fig. 2A, indices 3 and 4). There are a small number of histone mRNAs in S-phase cells which have more than 4 nt removed from the 3′ end, and many of these have longer U-tails added again restoring the length of the histone mRNA (Fig. 2A, indices 5 and 6).

There were dramatic changes at the 3′ ends of histone mRNAs in both the 3′hExo and TUT7 KO cell lines. In the TUT7 KO cell lines, more than half the HIST2HAA3 histone mRNAs had a tail shorter than 3 nt, and there were fewer uridylated tails present on the 3′ termini, with only about 20% as many nontemplated nucleotides added compared to WT cells (Fig. 2B,C). Only 84% of the nontemplated tails were uridines compared with >98% in the wild-type cells. Whether the presence of nontemplated nucleotides other than uridine is due to errors in sequencing or addition of other nucleotides to the histone mRNA cannot be determined. We did not observe significant levels of sequencing errors in the body of the mRNA, consistent with a small number of other nucleotides being added by other enzymes, resulting in a lower percentage of added nucleotides being uridine when TUT7 was knocked out. This result demonstrates that TUT7 is the primary enzyme responsible for adding uridines to the 3′ termini of histone mRNA. It is likely that TUT4, whose levels are increased in the TUT7 KO cells, is responsible for the addition of the uridines in the absence of TUT7, and that TUT4 is less efficient in uridylating histone mRNAs than TUT7.

The 3′hExo cell lines show an opposite pattern from the TUT7 KO cells (Fig. 2D). About half of the histone mRNAs

ended in a tail longer than 3 nt. There is still some trimming of the 3′ end, removing 1 or 2 nt, presumably by other exonucleases, but there are also 3′ ends ending in ACCCA or ACCC. A second difference is more extensive uridylation, with substantial amounts of ACCU and ACUU tails (which are included in the "longer" histone mRNAs), suggesting that TUT7 is still recruited to the histone mRNA to uridylate the mRNA in the absence of 3′hExo. The data are consistent with TUT7 and 3′hExo acting together to maintain the 3′ end with a 3 nt tail after the stem–loop. If more uridines are added by TUT7, they are then likely removed by 3′hExo.

The pie charts show that >80% of the HIST2HAA3 histone mRNAs in the wild-type cells end 3 nt after the stem–loop, either in ACC, ACU, AUU (Fig. 2A,B). In contrast in the TUT7 KO cells, more than half of the HIST2HAA3 mRNAs have a short tail (<3 nt), due to failure to uridylate trimmed mRNA (Fig. 2C). A similar pattern is seen for the HIST1H2BF mRNA with more than 90% of the mRNAs ending 3 nt after the stem–loop which is reduced to 70% in the TUT7 KO. The difference between the two genes is due to the large percentage of HIST1H2BF mRNAs that end in ACC. HIST2HAA3 is the longest histone mRNA in the cell with 67 nt between the stop codon and the stem–loop compared with 28 nt for HIST1H2BF, likely making it more sensitive to exonuclease trimming. In the 3′hExo KO cells, 40%–45% of the histone mRNAs in both genes have a tail longer than 3 nt, compared to <5% in WT cells with uridines added at index 2 (ACCU) or multiple uridines added at index 3 (ACUU) (Fig. 2D), and these are included in the "long" histone mRNAs in the pie charts.

The 3′ end of histone mRNA is the element that determines rapid degradation of histone mRNA when DNA replication is inhibited (Pandey and Marzluff 1987). The initial step in degradation is degradation into the stem (Mullen and Marzluff 2008; Hoefig et al. 2013), followed by extensive uridylation of nucleotides in the 3′ side of the stem (Slevin et al. 2014; Meaux et al. 2018). To investigate the effect of the knockouts on degradation, we treated the KO cell lines in mid-S-phase with hydroxyurea to stop DNA replication, which normally triggers the rapid degradation of histone mRNAs. We used northern blotting to visualize and quantify the degradation of the histone mRNA over the course of 40 min. In WT cells the histone mRNAs are degraded rapidly, with 90% of the mRNA degraded in 40 min. In TUT7 KO cells, the histone mRNAs were still degraded although the degradation rate was slower, with 25% of the histone mRNA remaining after 40 min (Fig. 3B). In contrast in the 3′hExo KOs, histone mRNAs were stable, with little or no degradation even 40 min after treatment with hydroxyurea (Fig. 3B). These results show that 3′hExo is essential for rapid degradation of histone mRNA, as previously demonstrated by Hoefig and coworkers in fibroblasts from 3′hExo knockout mice (Hoefig et al. 2013).

Degradation intermediates in the 3′hExo and TUT7 KO's

To assess the effect of the knockouts on the intermediates in histone mRNA degradation, we prepared EnD-seq

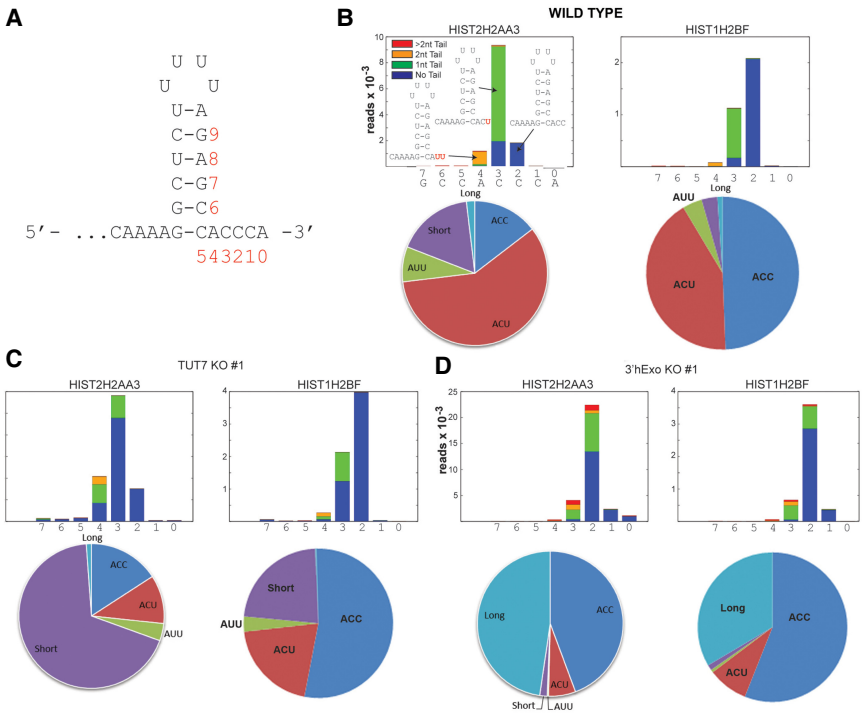

FIGURE 2. Analysis of the 3′ ends of the histone mRNAs in the KO cells. (*A*,*B*) The structure of the 3′ end of histone mRNA formed by 3′ processing in the nucleus. The 3′ ends of histone mRNAs were determined by the End-seq protocol with the results plotted as previously described (Welch et al. 2015). The position of the last templated nucleotide in the histone mRNA is indicated. 3′hExo removes 2 nt from the 3′ end of the processed histone mRNA. If more nucleotides are removed, a terminal uridyl transferase (TUTase) adds uridines back to the 3′ end with the number of uridines added indicated by the colored blocks. The structure of the three most abundant 3′ ends is shown. The pie chart shows the percentage of reads with the different 3′ ends in the HIST2HAA3 gene, with short and long indicating the amounts of the 3′ ends that were either shorter or longer than the major forms (ACC, ACU, and AUU) which extend 3 nt past the base of the stem. The results for two different histone mRNAs are shown. (*C*,*D*) The same analysis was performed for the TUT7 KO cells (*C*) and for the 3′hExo KO cells (*D*). The *y*-axis gives the number of reads for each index ($\times 10^{-3}$).

libraries after treatment of cells with hydroxyurea. In wild-type cells, there are two predominant sets of 3′ to 5′ degradation intermediates: the first is the result of degradation into the 3′ side of the stem–loop while SLBP is still bound, and uridylation of those RNAs, and the second is intermediates that accumulate starting 17 nt 3′ of the stop codon when the exosome would contact a paused terminating ribosome (Fig. 3A; Slevin et al. 2014; Meaux et al. 2018). Multiple intermediates are also detected as a result of further degradation into the ORF, which is still bound by ribosomes (Slevin et al. 2014). Lsm1–7, which binds to the U-tails on the intermediates in the stem, is also required for rapid degradation of histone mRNA (Mullen and Marzluff 2008; Lyons et al. 2014). There are very few intermediates between these two primary sets of intermediates in wild-type cells, suggesting that once degradation is initiated on the uridylated intermediates in the stem, 3′ to 5′ degradation by the exosome of the 3′-UTR occurs very rapidly, likely due to the removal of SLBP from the histone mRNA. There is extensive uridylation of both sets of intermediates in wild-type cells, with long U-tails (>5 nt) accumulating primarily on the GAG (indices 7 to 9) on the 3′ side of the stem–loop (Fig. 3C), as well as uridylation of the intermediates near the stop codon and in the ORF (Fig. 3C).

In the TUT7 knockouts, the pattern of degradation intermediates is strikingly different from control cells. There are almost no uridylated intermediates in the stem of the HIST2HAA3 mRNA compared with the wild-type RNA, with only small amounts of mono-uridylation at positions 7–9 (Fig. 3D). There are many more intermediates resulting from degradation further into the stem, which also are not uridylated, compared to wild-type cells. Figure 3C,D present the data as percent of intermediates in the stem–loop relative to the total reads (including the undegraded RNA) from samples with 40%–60% of the intact histone mRNA remaining, and plotted the data as percent of total reads at each nt. Because the pattern of degradation intermediates does not change as degradation proceeds (Meaux et al. 2018), the pattern represents the steady-state distribution of intermediates during degradation. The accumulation of large numbers of intermediates in the stem–loop in the TUT7 KOs suggests that the lack of uridylation results in failure to rapidly degrade through the stem–loop. The change in degradation intermediates in the stem–loop is qualitatively similar in HIST2HAA3 and HIST1H2BF

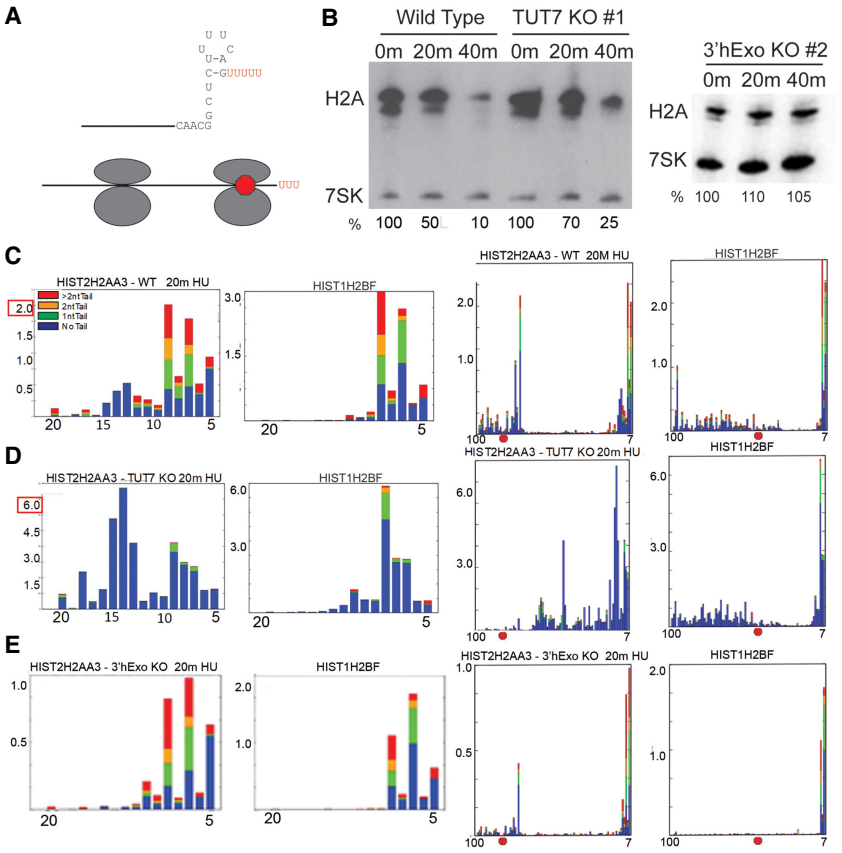

FIGURE 3. Effect of KO of TUT7 and 3′hExo on histone mRNA degradation. (*A*) Diagram of the two major classes of degradation intermediates in histone mRNA. The initial step is degradation 3′ to 5′ by 3′hExo into the stem where there is extensive uridylation of the intermediates. A second phase is rapid degradation until the exosome nears the terminating ribosome, resulting in an intermediate about 15 nt 3′ of the stop codon (red octagon). There is then slower degradation through the ORF of the mRNA with uridylation of many intermediates. (*B*) S-phase cells (3 h after release from double thymidine block) were treated with 5 mM hydroxyurea (HU) and RNA isolated from untreated cells, 20 and 40 min after treatment with HU. RNA was analyzed by northern blotting for the histone H2a mRNAs. 7SK RNA was measured as a loading control. The amount of histone mRNA was determined by PhosphorImager analysis with 7SK as the control. In the experiment with the 3′hExo KO, a different preparation of 7SK probe was used which had a higher specific activity than the probe used on the *left* panel for the TUT7 KO. (*C–E*) Libraries containing histone mRNAs were prepared from the WT, TUT7 KO, and 3′hExo KO cells 20 min after HU treatment, as previously described (Welch et al. 2015). The results for the 3′ end of two histone mRNAs, HIST2HAA3 which has a long 3′-UTR and HIST1H2BF which has a short 3′-UTR, are shown. The *left* panel shows the intermediates in the stem (nts 5–20), which were plotted showing the amount of uridylation of each intermediate as in Figure 2. The *right* panel plots the intermediates from 7–100. The position of the stop codon in each gene is shown by the red octagon. The *y*-axis shows the percentage of the intermediates relative to the total histone mRNA. Thus there are about 3× as many intermediates in the H2AA3 TUT7 library as in the wild-type library, and half as many intermediates in the 3′hExo library.

mRNAs, although the exact pattern of degradation intermediates is different (Fig. 3D).

The biggest difference is in the degradation intermediates in the HIST2HAA3 mRNA in the TUT7 KO cells between the stem and the stop codon. In the HIST2HAA3 mRNA, there is slow degradation through the region in the TUT7 KO resulting in a large number of intermediates, which are not found in WT cells. This long region is GC-rich which likely impedes degradation in the absence of TUT7. In the HIST1H2BF gene, which has the shortest region between the stem–loop and the stop codon, there are few intermediates in this region. In the HIST2HAA3 gene, there is a sixfold reduction in uridylation of the intermediates between the stop codon and the stem–loop or in the ORF, indicating that TUT7 is also important for these uridylations. In contrast, the uridylation in the stem–loop is reduced >90% in the stem–loop in both the HIST2HAA3 mRNA and the HIST1H2BF mRNAs (Table 1; Fig. 3D).

In the 3′ hExo knockouts, there were only small amounts of intermediates (Fig. 3E) resulting from degradation into the stem–loop. These were heavily uridylated. The small amount of degradation that occurs is likely due to other exonucleases initiating digestion of a small number of histone mRNAs into the stem, which are rapidly degraded and do not result in changing the steady-state level of the histone mRNA (Fig. 3B). The nuclease(s) responsible for this initial degradation in the absence of 3′hExo are not known. There is a lack of degradation intermediates between the stem–loop and the rest of the mRNA. Clearly the step that allows degradation to proceed into the 3′ side of the stem is impaired in the 3′hExo mutants, but if it does occur, then these intermediates are uridylated and rapidly degraded.

Cell-cycle analysis of 3′hExo and TUT7 knockouts

Histone mRNAs are degraded by the same 3′ to 5′ pathway at the end of S-phase as when DNA replication is inhibited in mid-S-phase (Meaux et al. 2018). We synchronized cells by double-thymidine block and determined the progression of cells through S-phase by measuring DNA content as well as by labeling cells for 30 min with EdU prior to harvesting to determine the rate of DNA synthesis. Both the wild-type cells and TUT7 KOs went through S-phase with similar kinetics (Fig. 4A; Supplemental Fig. S1). Histone mRNA levels were high in mid-S-phase and declined as cells exited S-phase (Fig. 4B). However, the levels of histone mRNA may decline more slowly in the TUT7 KO cells than in the wild-type cells (Fig. 4B), consistent with the slightly slower rate of degradation of histone mRNA seen in these cells after treatment with inhibitors of DNA replication in S-phase (Fig. 3B).

In contrast to the TUT7 KO cells, the 3′hExo cells progressed more slowly through S-phase. They were still in S-phase at 7–8 h and didn't undergo mitosis until 11–12 h, about 2 h later than the TUT7 KO or WT cells (Fig. 4A). Although the 3′hExo KO cells were delayed in leaving S-phase, and histone mRNA is not degraded in these cells even after 40 min of inhibition of DNA synthesis (Fig. 3B), the histone mRNA was still reduced to much lower levels before the cells underwent mitosis (Fig. 4B).

To analyze 3′ to 5′ degradation in cells at the end of S-phase, we analyzed degradation intermediates using the AppEnD workflow (Welch et al. 2015). As previously reported (Meaux et al. 2018), wild-type cells exiting S-phase 6 h after release from the double thymidine block showed a similar pattern of degradation intermediates to the hydroxyurea treated samples (Figs. 3C, 4C). The TUT7 KO cell lines exiting S-phase at 7 h also showed a similar pattern of degradation intermediates as was found after inhibition of DNA replication in S-phase in these cells, with almost no uridylation, and more intermediates throughout the stem–loop and into the 3′-UTR (Figs. 3D, 4D). As the 3′hExo KO cells were degrading histone mRNAs in G2 (10 h, Fig. 4B), we analyzed the degradation intermediates at the 3′ end at this time point. There were only a small number of degradation intermediates initiated from the 3′ end (note scale in Fig. 4E) compared to WT S-phase cells treated with HU (Fig. 3E), or the TUT7 and WT KO cells at the end of S-phase. These intermediates were uridylated. The failure to observe large numbers of intermediates in degradation from the 3′ end at a time when the histone mRNA is being degraded, suggests that there is a different pathway leading to histone

TABLE 1. Effect of TUT7 KO on uridylation of histone mRNA degradation intermediates

		HIST2HAA3 tails ≥2			HIST1H2BF tails ≥2		
Cell line	Gene nucleotides	AVG	±SD	*P*-value	AVG	±SD	*P*-value
WT	6–20	34.85	2.0	0.0001	27.9	6.5	0.0001
TUT7		1.05	0.31		3.4	0.18	
WT	30–150	19.5	6.6	0.0001	11.6	1.07	0.01
TUT7		3.50	1.3		0.78	0.26	

The percentage of reads with U tails ≥2 in the stem–loop (nts 6–20, top) or between nts 30–150 (bottom) for wild-type cells or TUT7 KO cells was determined for the HIST2H2AA3 mRNA and the H2BF mRNA. The samples were S-phase cells treated with HU for 20 min or cells that were in G2 and rapidly degrading histone mRNA, and the results for these samples were combined. The results for the two TUT7 KO lines were combined (N = 4 for WT and N = 4 for TUT7).

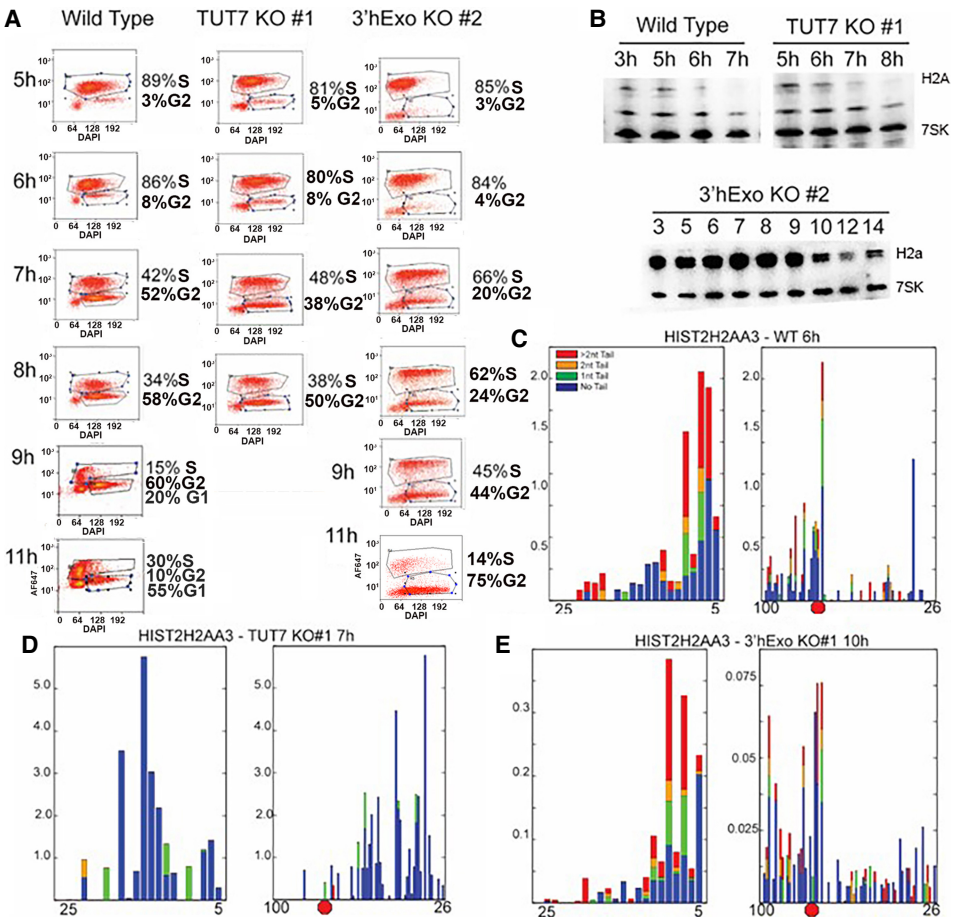

FIGURE 4. Histone mRNA metabolism during the cell cycle in the TUT7 and 3′hExo KO cells. (*A*) Flow cytometry analysis. Parallel cultures of the WT, TUT7, and 3′hExo KO cells were synchronized by double thymidine block and cells analyzed by flow cytometry starting 3 h after release. About 93% of the WT entered the cell cycle (note the number of cells that stayed arrested in the *bottom left*); about 88% of the TUT7 and 3′hExo cells entered the cell cycle. Samples were labeled with EdU for 30 min before harvesting to identify S-phase cells. The *y*-axis shows the intensity of EDU staining and the *x*-axis shows the amount total DNA determined by DAPI. A small number of cells do not reenter S-phase after release from the double thymidine block (*lower left* corner of flow cytometry distribution). (*B*) Northern blot of histone mRNAs as cells exit the cell cycle. This was from a different experiment than *A*, and in each experiment there were slight differences in the rate of progression of S-phase, and in every experiment, WT and TUT7 KO cells were synchronized in parallel. The results of this northern blot were used to determine the sample used in panels *C*–*E* for analysis of histone mRNA degradation intermediates. Note that the histone mRNA levels decrease slightly later in the TUT7 KO than in the WT cells. (*C*–*E*) Histone mRNA degradation intermediates in the WT cells, TUT7 KO cells and 3′hExo KO cells during the time histone mRNAs were being degraded (6 h, 7 h, and 10 h, respectively) are shown. The data were plotted as in Figure 3.

mRNA degradation in G2 cells in the 3′hExo KO cells, which is not active when DNA replication is inhibited in S-phase. We speculate that this pathway involves either 5′ to 3′ degradation or endonucleolytic cleavage and may serve as a back-up pathway for failure to degrade histone mRNAs at the end of S-phase.

Expression of 3′hExo or TUT7 rescues the KO phenotypes

To rescue the KO cells, we used lentiviral vectors to stably express either 3′hExo or TUT7 in the KO cells (Fig. 5A). TUT7 was expressed from the constitutively active EFS promoter (Shalem et al. 2014), and the ORF was fused to a puromycin resistance gene separated by a P2A cleavage peptide. We could not successfully generate stably transfected cells expressing 3′hExo using plasmid-based expression vectors, likely because overexpression of 3′hExo was harmful to the cells. Therefore, we cloned 3′hExo or catalytically dead 3′hExo into a TET-inducible lentiviral vector, with the puromycin resistance gene fused with the TET activator, separated by a T2A-cleavage peptide (Fig. 5A). We transduced KO cells and selected clones of puromycin resistant cells.

For the TUT7 KO cells, we selected clones that expressed TUT7 protein at a similar level to the wild-type cells (Fig. 5B; Supplemental Fig. S3). We tested these KO cells for the level of TUT4 expression, which was increased about fivefold in the TUT7 KO cells (Fig. 1E, 5C), and also tested the rescue clones for TUT4 expression. In

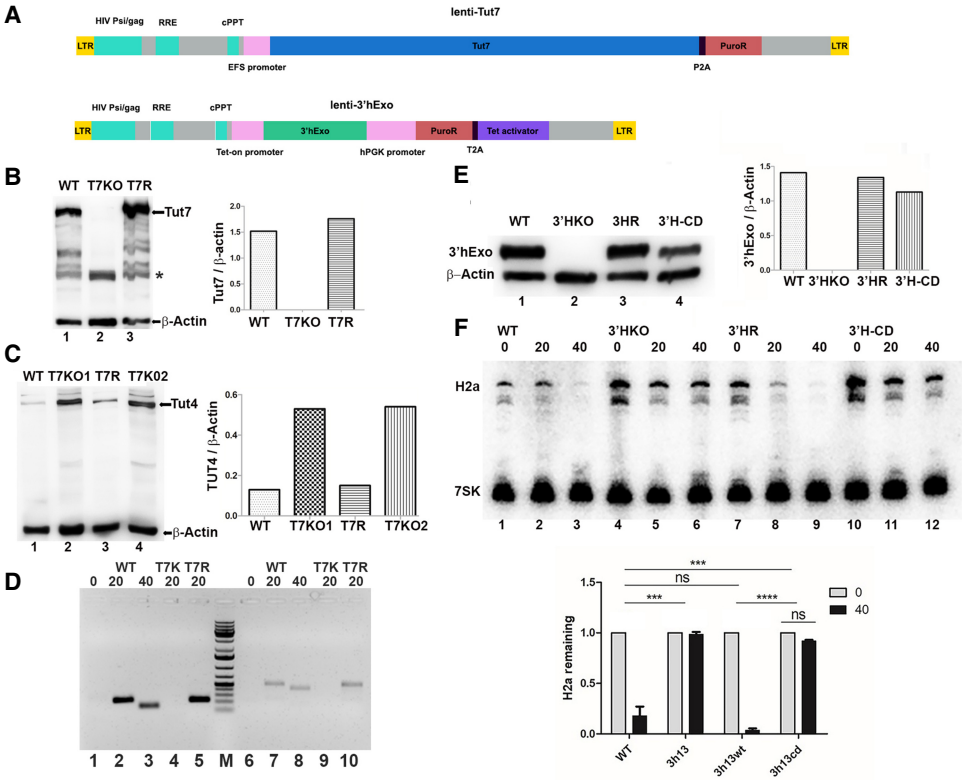

FIGURE 5. Rescue of the TUT7 and 3′hExo KO cells. (*A*) Schematic of lentiviral vectors used for expression of TUT 7 (*top*) and 3′hExo (*bottom*). The 3′hExo vector is TET inducible, and the TUT7 vector is not (since the size of the TUT7 ORF was too large to also include the TET regulatory system). (*B*) TUT7 KO cells were transduced with the lentiviral vector expressing TUT7. Clonal cell lines were isolated from puromycin resistant cells. A western blot WT (lane *1*), T7KO1 (lane *2*), and of a cell line expressing similar amounts of TUT7 as the WT cells in shown (lane *3*). The (*) indicates a cross-reacting band. Other bands in the WT and rescued cells are likely proteolytic products of TUT7. (*C*) Both the TUT7KO1 and TUT7KO2 cells were rescued with the lentiviral vector. The levels of TUT4 protein in the KO and rescued cells were determined by western blotting. The levels of TUT4 are increased in the KO cells and decreased to levels similar to the WT in the rescued cells. (*D*) The TUT7 rescue cells rescue the uridylation of histone mRNA degradation. Uridylated histone mRNA degradation intermediates were detected by RT-PCR using a reverse primer that ended in 3A's and a forward primer in two different histone H2a genes, as described in Mullen and Marzluff (2008). RNA from exponentially growing cells (lanes *1* and *6*) and cells treated for 20 (lanes *2* and *7*) or 40 min with HU (lanes *3* and *8*) was analyzed. RNA from the TUT7 KO cells (lanes *4* and *9*) and the TUT7 rescued cells (lanes *5* and *10*) after 20 min of HU treatment were analyzed to demonstrate the rescue of uridylation. (*E*) The 3′hExo KO cells were rescued using the lentiviral vector containing the TET-ON system expressing either the active or catalytically dead 3′hExo. Cloned cell lines were isolated and the levels of tetracycline necessary to restore close to normal expression of 3′hExo were determined (Supplemental Fig. S3A–D). Western blots showing 3′hExo levels in the WT, KO, and cells rescued with WT 3′hExo (3HR) or catalytically dead (3′H-CD) 3′hExo relative to the levels of actin are shown. (*F*) The levels of histone mRNA in the WT (lanes *1–3*), 3′hExoKO (lanes *4–6*), KO cells rescued with WT 3′hExo (lanes *7–9*), and KO cells rescued with catalytically dead 3′hExo (lanes *10–12*) before (lane *1,4,7,10*) and after treatment with HU for 20 (lanes *2,5,8,11*) or 40 (lanes *3,6,9,12*) minutes. Histone H2a mRNA levels were determined by northern blotting using the 7SK RNA as an internal control. The results of three independent experiments were quantified using a PhosphorImager.

the rescue clones the TUT4 expression was reduced to close to wild-type levels. Thus the compensatory increase in TUT4 expression observed in the TUT7 KO cells was reversed by the expression of TUT7 protein.

To demonstrate that the expression of TUT7 rescued the uridylation of the histone mRNA degradation intermediates, we used the approach we previously used to analyze histone mRNAs with ≥3 nt U-tails (Mullen and Marzluff 2008). We analyzed two different histone H2A mRNAs, priming cDNA synthesis with a primer ending with 3 A's at the 3′ end. WT cells, TUT7 KO cells and TUT7 rescue cells were treated with HU for 20 or 40 min. There was no detectable PCR product in untreated cells (Fig. 5D, lanes 1 and 6) or in TUT7 KO cells treated with HU for 20 min (Fig. 5D, lanes 4 and 9). Uridylated histone mRNAs were detected in WT cells after HU treatment (Fig. 5D, lanes 2,3,7,8) and in the TUT7 rescue cells treated with HU for 20 min (Fig. 5D, lanes 5 and 10). Thus TUT7 expression rescued the defect in histone mRNA degradation in the TUT7 KO cells.

For the 3′hExo rescue experiments, we tested the different cloned cell lines for the expression of 3′hExo after addition of different amounts of doxycycline and obtained conditions where the cells expressed each protein at close to wild-type levels (within a factor of 2) (Fig. 5E;

Supplemental Fig. S3C,D). The 3′hExo KO cells did not rapidly degrade histone mRNA when DNA replication was inhibited (Fig. 5F, lanes 4–6). However, expressing WT 3′hExo in the KO cells resulted in histone mRNA degradation being restored to a similar rate as in WT cells, with most of the mRNA degraded by 40 min (Fig. 5F, lanes 7–9). In contrast, the cells expressing the catalytically dead protein, D298A (Yang et al. 2006), which will still bind to the 3′ end of histone mRNA, degraded histone mRNA much more slowly, although there was more degradation than in the 3′hExo KO cells (Fig. 5F, lanes 10–12), as was also reported in previous studies in fibroblasts from 3′hExo KO mice (Hoefig et al. 2013).

We conclude the TUT7 and 3′hExo together function both to maintain the proper length of the 3′ end of histone mRNAs in S-phase cells, as well as participating in the rapid degradation into the stem–loop that occurs when histone mRNAs are rapidly degraded either by inhibition of DNA replication or at the end of S-phase. A model of the pathway of metabolism of histone mRNA in S-phase (Fig. 6A, panels a–c) and the proposed pathway of degradation of histone mRNA is shown in Fig. 6A (panels d–h), starting with degradation into the stem by 3′hExo. Figure 6B shows what we propose is the critical intermediate in histone mRNA degradation (between Fig. 6A, panels e and f), which is the intermediate from which SLBP is removed.

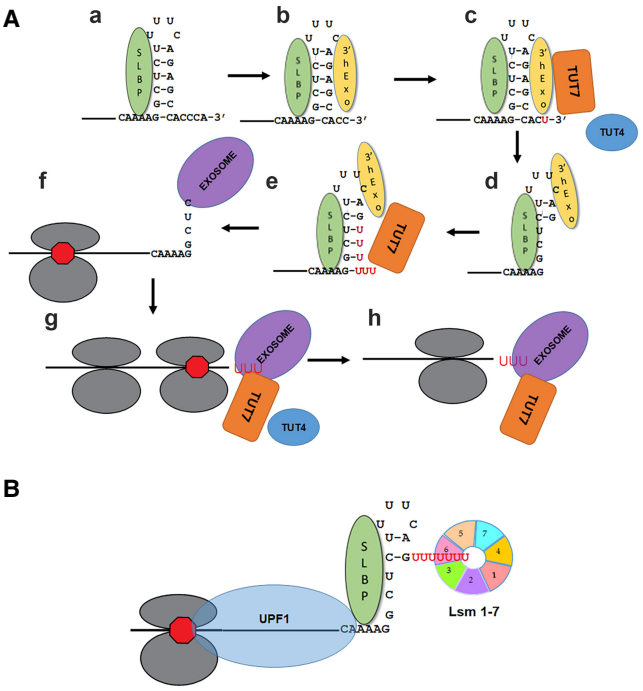

FIGURE 6. Model of histone mRNA degradation. (*A*) Role of TUT7 and 3′hExo in histone mRNA metabolism and degradation. (a–c) The processed histone mRNA has a 5 nt 3′ tail (a) which is trimmed by 3′hExo to 3 nts (b). If there is additional trimming, a TUTase adds uridine to restore tail to 3 nt (c). (d–h) When DNA synthesis is inhibited in S-phase or at the end of S-phase, 3′hExo degrades into the stem (d), and long U-tails are added by TUT7 (e). It is likely that repeated cycles of degradation and uridylation occur since intermediates at each nt are readily detected (Figs. 2–4). SLBP is removed and processive degradation, likely by the exosome, is activated (f). Degradation is stalled by the terminating ribosome and the RNA is uridylated (g). The exosome can proceed through the ribosome and then ultimately through the ORF with uridylated intermediates (h). Note that the initial intermediates with U-tails added in the stem likely can form a stem–loop with the U's pairing with the two G's on the 5′ side of the stem, which is then able to bind SLBP (PE Lackey and WF Marzluff, unpubl.). Once the U-tail is long enough to bind Lsm 1–7 then it can no longer bind SLBP. It is likely that TUT7 specifically interacts with the 3′ end of histone mRNA bound to SLBP to account for this specificity. (*B*) Schematic of the intermediate just before removal of SLBP (between e and f in panel *A*). Lsm 1–7 binds to long U-tails (>7 nt) added to intermediates in the stem, and interacts directly with SLBP and 3′hExo (Lyons et al. 2014). Together with Upf1, which is bound to the terminating ribosome and the 3′-UTR after inhibition of DNA replication, SLBP is removed, allowing processive degradation until the terminating ribosome is reached.

DISCUSSION

Uridylation of the 3′ ends of many types of RNAs are involved in the metabolism of the RNA. In many cases uridylation is part of the degradation mechanism, while in some cases uridylation stabilizes the RNA. For example, in let7-pre-miRNA addition of a single U at the 3′ end is essential for proper processing and production of functional let-7 miRNA, while addition of longer U tails is required for its degradation (Kim et al. 2015). "Deadenylated mRNAs," which have the bulk of the poly(A) tail removed but retain a short A tail, are also subject to uridylation (Chang et al. 2014). The function of this uridylation is less clear, with evidence that uridylation can stabilize the mRNAs in plants (Zuber et al. 2016), while uridylation of the deadenylated mRNAs accelerates the degradation of mRNA in yeast (Rissland and Norbury 2009) and mammals (Lim et al. 2014). There are two major cytoplasmic uridyl transferases, TUT7 and TUT4 (TENT3A and TENT3B; ZCCHC6 and ZCCHC11). For the uridylation of pre-miRNAs, miRNAs, damaged structural RNAs, and most polyadenylated mRNAs, either TUT4 or TUT7 can function in vivo.

TUT7 is the uridyl transferase that maintains the 3′ tail of histone mRNAs during S-phase

Mammalian replication-dependent histone mRNAs, which are formed by an endonucleolytic cleavage 5 nt after the stem–loop, also show two types of uridylation. A ternary complex consisting of SLBP and 3′hExo forms on the 3′ end of histone mRNA after processing. 3′hExo can remove 2 nt, resulting in the major form of cytoplasmic histone mRNA ends 3 nt after the stem–loop (Mullen and Marzluff 2008). We find that TUT7 is the primary uridyl transferase that modifies histone mRNA to maintain the 3 nt tail after the SL. If 3′hExo removes additional nucleotides, then TUT7 can restore the 3 nt tail by adding

uridines, an example of uridylation adding nucleotides to maintain the function of histone mRNA. We show that most of these tails are added by TUT7, but there is some (~20%) residual uridylation in the TUT7 KO's, which may be done by TUT4 (Fig. 2). In the TUT7 KOs, histone mRNAs are overall shorter than in WT S-phase cells. Note that TUT7 is still recruited to the 3′ end of the histone mRNA in the absence of the 3′hExo since more extensive uridylation occurs in 3′hExo KO cells, and the histone mRNAs are longer than in WT cells. Thus, there is normally a balance of uridylation and 3′ to 5′ exonuclease activity of 3′hExo, to maintain a 3 nt tail after the SL of histone mRNA.

Tut7 is the uridyl transferase that functions in the initial steps of histone mRNA degradation

When DNA synthesis is inhibited, histone mRNAs are rapidly degraded, with 3′ hExo essential for rapid degradation. It degrades the 3′ end into the 3′ side of the stem–loop, and longer U tails are added to the degradation product on the 3′ side of the stem (Slevin et al. 2014; Meaux et al. 2018). These longer U-tails can then bind Lsm1–7, triggering rapid degradation of the initial intermediates (Lyons et al. 2014). In the TUT7 KO cells degradation is initiated into the stem, but there are essentially no U tails added, indicating that TUT7 is specifically required for this modification.

There must be a change in the structure of the SLBP/SL/RNA complex when degradation is initiated allowing 3′hExo to degrade into the stem–loop, since there is no change in 3′hExo levels during the cell cycle. A major change that occurs at this time is the recruitment of Upf1 to the histone mRNA, likely binding to the stop codon and the 3′-UTR up to the stem–loop. The helicase activities of Upf1 and Smg1 are also required (Kaygun and Marzluff 2005a; Meaux et al. 2018). What the signal is that recruits Upf1 is not known.

Once degradation has proceeded past the stem–loop, there is rapid degradation of the 3′-UTR up to close to the stop codon where degradation intermediates accumulate likely because there is a ribosome still bound at the stop codon. Together these results strongly suggest that TUT7 is specifically recruited to the SLBP/3′hExo/SL complex, is essential for the degradation into the stem–loop, and important for uridylating additional intermediates. A recent study found that the exosome is capable of degrading mRNA bound to ribosomes 3′ to 5′ (Kogel et al. 2022) and a global analysis of RNA degradation in mouse ES cells implicating the exosome in degradation of histone mRNAs (Tuck et al. 2020), consistent with the exosome being the nuclease that degrades histone mRNA once SLBP is removed.

A critical step in histone mRNA degradation is likely the removal of SLBP from the mRNA, which likely occurs after degradation and extensive uridylation of the stem–loop, resulting in the recruitment of Lsm1–7. The complex, containing Upf1, Lsm1–7, SLBP bound to histone mRNA (Fig. 6B; Lyons et al. 2014; Kaygun and Marzluff 2006; Meaux et al. 2018) likely participates in removal of SLBP and also recruitment of the exosome, leading to rapid degradation through the 3′-UTR close to the terminating ribosome.

Effect of KO of TUT7 on histone mRNA degradation

In the absence of Tut7, there is only a small change in the overall rate of degradation of histone mRNA and no change in the progression through the cell cyle. There is a change in the pattern of histone mRNA degradation intermediates with approximately threefold increase in the intermediates in the stem–loop, and accumulation of intermediates further into the stem–loop than in WT cells. This result is consistent with 3′hExo continuing to degrade the histone mRNA due to failure to efficiently recruit the exosome. Strikingly, in the HIST2HAA3 mRNA, which has the longest 3′-UTR of the RD (replication-dependent) histone genes, and which is very GC-rich, large numbers of intermediates (not found in the WT cells) accumulate in the 3′-UTR, consistent with the possibility that 3′ hExo is slowly degrading this region, until the exosome is ultimately recruited to degrade the ORF. The overall rate of histone mRNA degradation was only slightly slower than in wild-type cells, although the histone mRNAs were degraded both after inhibition of DNA replication in S-phase and at the end of S-phase. In histone mRNAs with shorter 3′-UTRs that are not GC-rich, for example, H2BC4, degradation proceeded efficiently through this region.

3′hExo KO slows progression though S-phase

The 3′hExo KOs progress more slowly through S-phase (with lower levels of histone mRNA consistent with a lower rate of DNA replication), taking about 2 h longer to complete S-phase. The reason for this is not known. Histone mRNA levels remain high as cells enter G2 but histone mRNAs are degraded prior to mitosis. The pathway of degradation differs from the normal degradation at the end of S-phase, since we did not find increased levels of 3′ to 5′ degradation intermediates during this time, but rather a low number of intermediates similar to that found when S-phase 3′hExo KO cells were treated with HU and histone mRNA concentrations remained constant. This result suggests that histone mRNAs are degraded by a different mechanism in the 3′hExo KO cells prior to mitosis, possibly 5′ to 3′ degradation. 5′ to 3′ degradation intermediates would not have been detected by our approach. Degradation of histone mRNA prior to mitosis in the 3′hExo KOs may be a "back-up" strategy to assure degradation of histone mRNAs before cell division.

TUT7 KO cells express more TUT4 protein

Both TUT7 KOs contained more TUT4 protein than wild-type cells, an increase of about fourfold. Stably expressing TUT7 in the KO cells resulted in a reduction in TUT4 levels close to that in wild-type cells, indicating that the TUT4 increase is a reversible compensatory response to the loss of TUT7. Note that this increase was not observed in RNAi experiments where TUT7 was knocked down (Lackey et al. 2016). Since this increase in TUT4 does not rescue the uridylation of the histone mRNA intermediates, it may be that there are essential TUT7 uridylation events that can only be compensated for by an increase in TUT4 levels. Alternatively, the increase in TUT4 might indicate a need for increased total uridylation activity as a result of the TUT7 KO.

MATERIALS AND METHODS

Cell culture and transfection

All experiments were performed in HCT116 colon carcinoma cells with McCoy's 5A medium (Corning, 10-050-CV). 400k cells were seeded in six-well plates on day 0, and on day 1 three different plamids (GFP, gRNA expressing plasmid, Cas9, 500 ng/plasmid) were transfected with Lipofectamine 2000 (Thermo Fisher) into the cells. Three days later, GFP positive cells were selected by flow cytometry. For cell-cycle experiments, cells were synchronized with double thymidine block. Cells were treated with thymidine (final concentration 2 mM) in six-well plates for 12 h. Cells were then washed with PBS and fresh media and allowed to grow for 9 h. A second thymidine block (2 mM) was added for another 12 h. Cells were then washed again with PBS and allowed to grow in thymidine-free media. Time points from the start of S-phase were taken starting at the second release. For study of histone mRNA degradation, cells were treated with 5 mM hydroxyurea (HU) 3 h into S-phase, incubated for an additional 20 and 40 min and total cell RNA prepared for analysis of histone mRNA degradation. Parallel wells were also collected for protein analysis by washing cells with PBS and treating with 500 µL of trypsin. Samples were run on 10% SDS PAGE for 3′hExo samples and 6% SDS PAGE for TUT7 samples. Antibodies for TUT7 (Proteintech, 25196-1; 1:1000 dilution), TUT4 (Proteintech, 18980-1; 1:500 dilution), 3′hExo (Dominski et al. 2003; 1:3000), and the loading control β-Actin (GeneTex, #41554; 1:10,000) or PTB (a gift from Mariano Garcia-Blanco; 1:1200) were used in 5% milk and PBST.

CRISPR design

Two sgRNAs (TUT7-sgRNA1: GTGGCTGTCATTCATCCAAG; TUT7-sgRNA2: TGGCTGTCTGATGAACATAC 3′hExo-sgRNA: ACTGAAGTCACTCGCACTGG) were designed to target Exon 2 of TUT7 downstream from the start codon, and one sgRNA was designed to target exon 2 of 3′hExo. Synthetic sgRNA oligos containing a 5′ phosphate (Integrated DNA Technologies) was ligated to the sgRNA vector (Addgene, #51133) digested with BsaI. Guide plasmids were transfected in equal mass with a FLAG-tagged CAS9 expression plasmid (Addgene, #44758) and a GFP expressing plasmid (pmaxGFP from Lonza). Cells were sorted 3 d after transfection by FACS to produce three 96-well plates of single cells expressing GFP. The mutations were detected by genomic PCR and sequenced as previously described (He et al. 2018). Briefly, primers were designed (PRIMER3) 500 bp around the target genome sequences and the correct PCR products were sequenced (Eton Bioscience) to detect mutations. In order to determine the exact sequence of each allele, the potentially correct PCR products were cloned into pBlueScript II and sequenced (TUT7-sequenceR: GCTGACTCTGGGGTTGTGAT; 3′hExo: CATTGCCGGTAGGTCATTAAA).

Preparation of samples for high-throughput sequencing

RNA was extracted and treated with DNase as previously described and then applied to make libraries as described (Holmquist and Marzluff 2019). Briefly, the RNA was linked to a linker oligonucleotide and then reverse-transcribed to cDNA from the known 3′ linker sequence. Two rounds of PCRs were used to amplify the target sequence using the same linker primer and histone specific primers except for adding the Illumina adapters to the primers for the second round PCR. The samples were sequenced on an Illumina MiSeq using a MiSeq Reagent Kit v3.

Mapping EnD-seq data

Libraries were mapped to hg19 to identify the specific nucleotides on the 3′ terminus and any additional nontemplated nucleotides that were added. The data was analyzed with the AppEnD workflow (Welch et al. 2015).

Flow cytometry

During synchronization, cells were treated with 100 µM of EdU 30 min prior to harvesting time points for synchronizing cells. After fixed in 4% formaldehyde for 15 min, cells were washed in a solution of 1% BSA and then resuspended in a solution of 1% BSA and 0.5% Triton X-100 for 15 min. Cells were pelleted and then labeled with 500 µL of a solution of 1 mM $CuSO_4$, 1 µM Alexa Fluor 647 Azide, 100 mM ascorbic acid for 30 min in foil. An amount of 1 mL of 1% BSA and 0.5% Triton X-100 was added and then cells were pelleted. Cells were resuspended in 500 µL of 1% BSA, 0.5% Triton X-100, 1:1000 DAPI, and 40 µg/mL RNase, and then incubated with DAPI in the dark for 1 h at 37°C before filtering and running on a CYAN Flow Cytometer. The *y*-axis is read as the logarithm of intensity at 647 nm, and the *x*-axis is read as the DAPI area. A total of 10,000 events were collected for each time point.

Lentiviral stable cell line generation

The pCW57.1 plasmid was a gift from David Root (Addgene, #41393). 3′hExo cDNA was cloned into pCW57.1 using NheI and AgeI. Site-directed mutagenesis was then used to generate the catalytically dead mutant 3′hExo. The lentiCRISPRv2 plasmid was a gift from Feng Zhang (Addgene, #52961) (Sanjana et al. 2014). This plasmid was modified by removing the hU6-sgRNA

cassette and removing Cas9 to create an empty lenti-EFS cloning vector. TUT7 cDNA was cloned into lenti-EFS using AgeI and BamHI. Recombinant lentivirus was produced via triple plasmid transfection with pSPAX2 and VSVg glycoprotein for pseudotyping in HEK293 cells (Sanjana et al. 2014). Media supernatant was harvested at 48 h post transfection and filtered. The appropriate knockout cell lines were seeded at 100% confluency in a six-well plate and incubated with 8 µg/mL polybrene (Millipore, TR-1003) and lentiviral supernatant for 15 min in six-well plates. The cells were then spun down for 30 min at 400*g* at room temperature, and media changed after 2–4 h. Forty-eight hours post infection, cells were selected with puromycin, and were maintained in puromycin during the experiments.

We picked single cell colonies from each transduction. For the TUT7 expression, we determined expression by western blotting and selected clones which gave similar expression as the wild-type cells. For the 3′hExo expression, we cloned single cells and tested the colonies for failure to express 3′hExo in the absence of doxycycline. These colonies were then analyzed after growth for 3 d in the presence gradient concentration of doxycycline to determine the volume of doxycycline which induces expression of 3′hExo similar to wild-type (Supplemental Fig. S3). We used 100 ng/mL doxycycline for the 3′HR and 50 ng/mL for the 3′HCD to express amounts of 3′hExo similar to that in wild-type cells.

RNA analysis

Northern blotting was performed as previously described (Potter-Birriel et al. 2021). Briefly, total RNA was collected after HU treatment, extracted by TRIzol and quantified by NanoDrop. An amount of 2 µg of total RNA was loaded with RNA loading dye (NEB) on a 6% acrylamide-8M gel with 1xTris, borate and EDTA buffer (TBE) and then transferred to the membrane. After drying, the membrane was UV crosslinked and hybridized with probes to histone mRNA(H2a) and 7SK as control RNA. The probe was made according to the manufacturer's instructions (Agilent, #300385). The RNA was detected by a PhosphorImager and analyzed with GraphPad Prism (version 9.3).

Western blot

Cells were collected after HU treatment and washed once with cold 1× PBS, then suspended in 0.5% NP40 lysis buffer for 20 min on ice, centrifuged 20 min at 12,000 rpm at 4°C. The supernatants were saved and quantified using Bio-Rad protein assay dye (Bio-Rad, #5000006) by BioPhotometer (Eppendorf). An amount of 10 µg protein was loaded on an SDS-8% polyacrylamide gel and transferred to a nitrocellulose membrane (Thermo Fisher). After blocking in 5% milk in 1× PBS, incubating with primary and secondary antibody, the protein was detected by Kwik Quant Imager system.

DATA DEPOSITION

Sequencing data has been deposited in GEO (GSE203392).

SUPPLEMENTAL MATERIAL

Supplemental material is available for this article.

ACKNOWLEDGMENTS

This work was supported by grant GM29832 from the National Institute of General Medical Sciences (NIGMS) to W.F.M. We thank Dr. Chelsea Raulerson for assistance with the bioinformatics, and members of the Marzluff laboratory for advice and discussions.

Received June 7, 2022; accepted August 12, 2022.

REFERENCES

Brattain MG, Marks ME, McCombs J, Finely W, Brattain DE. 1983. Characterization of human colon carcinoma cell lines isolated from a single primary tumour. *Br J Cancer* **47:** 373–381. doi:10.1038/bjc.1983.56

Chang H, Lim J, Ha M, Kim VN. 2014. TAIL-seq: genome-wide determination of poly(A) tail length and 3′ end modifications. *Mol Cell* **53:** 1044–1052. doi:10.1016/j.molcel.2014.02.007

Chang H, Yeo J, Kim JG, Kim H, Lim J, Lee M, Kim HH, Ohk J, Jeon HY, Lee H, et al. 2018. Terminal uridylyltransferases execute programmed clearance of maternal transcriptome in vertebrate embryos. *Mol Cell* **70:** 72–82.e77. doi:10.1016/j.molcel.2018.03.004

Dominski Z, Yang X, Kaygun H, Marzluff WF. 2003. A 3′ exonuclease that specifically interacts with the 3′ end of histone mRNA. *Mol Cell* **12:** 295–305. doi:10.1016/S1097-2765(03)00278-8

Faehnle CR, Walleshauser J, Joshua-Tor L. 2017. Multi-domain utilization by TUT4 and TUT7 in control of let-7 biogenesis. *Nat Struct Mol Biol* **24:** 658–665. doi:10.1038/nsmb.3428

Graves RA, Pandey NB, Chodchoy N, Marzluff WF. 1987. Translation is required for regulation of histone mRNA degradation. *Cell* **48:** 615–626. doi:10.1016/0092-8674(87)90240-6

Harris ME, Böhni R, Schneiderman MH, Ramamurthy L, Schümperli D, Marzluff WF. 1991. Regulation of histone mRNA in the unperturbed cell cycle: evidence suggesting control at two posttranscriptional steps. *Mol Cell Biol* **11:** 2416–2424. doi:10.1128/mcb.11.5.2416-2424.1991

He WX, Wu M, Liu Z, Li Z, Wang Y, Zhou J, Yu P, Zhang XJ, Zhou L, Gui JF. 2018. Oocyte-specific maternal Slbp2 is required for replication-dependent histone storage and early nuclear cleavage in zebrafish oogenesis and embryogenesis. *RNA* **24:** 1738–1748. doi:10.1261/rna.067090.118.

Hoefig KP, Rath N, Heinz GA, Wolf C, Dameris J, Schepers A, Kremmer E, Ansel KM, Heissmeyer V. 2013. Eri1 degrades the stem-loop of oligouridylated histone mRNAs to induce replication-dependent decay. *Nat Struct Mol Biol* **20:** 73–81. doi:10.1038/nsmb.2450

Holmquist CE, Marzluff WF. 2018. Determining degradation intermediates and the pathway of 3′ to 5′ degradation of histone mRNA using high-throughput sequencing. *Methods* **155:** 104–115. doi:10.1016/j.ymeth.2018.11.001

Holmquist CE, Marzluff WF. 2019. Determining degradation intermediates and the pathway of 3′ to 5′ degradation of histone mRNA using high-throughput sequencing. *Methods* **155:** 104–115. doi:10.1016/j.ymeth.2018.11.001

Kaygun H, Marzluff WF. 2005a. Regulated degradation of replication-dependent histone mRNAs requires both ATR and Upf1. *Nat Struct Mol Biol* **12:** 794–800. doi:10.1038/nsmb972

Kaygun H, Marzluff WF. 2005b. Translation termination is involved in histone mRNA degradation when DNA replication is inhibited. *Mol Cell Biol* **25:** 6879–6888. doi:10.1128/MCB.25.16.6879-6888.2005

Kaygun H, Marzluff WF. 2006. Upf1 functions in regulation of mammalian histone mRNA decay. In *Nonsense-mediated mRNA decay* (ed. Maquat LE), pp. 237–252. Landes Bioscience, Georgetown, TX.

Kim B, Ha M, Loeff L, Chang H, Simanshu DK, Li S, Fareh M, Patel DJ, Joo C, Kim VN. 2015. TUT7 controls the fate of precursor microRNAs by using three different uridylation mechanisms. *EMBO J* **34:** 1801–1815. doi:10.15252/embj.201590931

Kogel A, Keidel A, Bonneau F, Schafer IB, Conti E. 2022. The human SKI complex regulates channeling of ribosome-bound RNA to the exosome via an intrinsic gatekeeping mechanism. *Mol Cell* **82:** 756–769.e758. doi:10.1016/j.molcel.2022.01.009

Labno A, Warkocki Z, Kulinski T, Krawczyk PS, Bijata K, Tomecki R, Dziembowski A. 2016. Perlman syndrome nuclease DIS3L2 controls cytoplasmic non-coding RNAs and provides surveillance pathway for maturing snRNAs. *Nucleic Acids Res* **44:** 10437–10453.

Lackey PE, Welch JD, Marzluff WF. 2016. TUT7 catalyzes the uridylation of the 3′ end for rapid degradation of histone mRNA. *RNA* **22:** 1673–1688. doi:10.1261/rna.058107.116

Lim J, Ha M, Chang H, Kwon SC, Simanshu DK, Patel DJ, Kim VN. 2014. Uridylation by TUT4 and TUT7 marks mRNA for degradation. *Cell* **159:** 1365–1376. doi:10.1016/j.cell.2014.10.055

Lyons SM, Ricciardi A, Guo AY, Kambach C, Marzluff WF. 2014. The C-terminal tail of Lsm4 interacts directly with the 3′ end of the histone mRNP and is required for efficient histone mRNA degradation. *RNA* **20:** 88–102. doi:10.1261/rna.042531.113

Marzluff WF, Wagner EJ, Duronio RJ. 2008. Metabolism and regulation of canonical histone mRNAs: life without a poly(A) tail. *Nat Rev Genet* **9:** 843–854. doi:10.1038/nrg2438

Meaux SA, Holmquist CE, Marzluff WF. 2018. Role of oligouridylation in normal metabolism and regulated degradation of mammalian histone mRNAs. *Philos Trans R Soc Lond B Biol Sci* **373:** 20180170. doi:10.1098/rstb.2018.0170

Morgan M, Much C, DiGiacomo M, Azzi C, Ivanova I, Vitsios DM, Pistolic J, Collier P, Moreira PN, Benes V, et al. 2017. mRNA 3′ uridylation and poly(A) tail length sculpt the mammalian maternal transcriptome. *Nature* **548:** 347–351. doi:10.1038/nature23318

Morgan M, Kabayama Y, Much C, Ivanova I, Di Giacomo M, Auchynnikava T, Monahan JM, Vitsios DM, Vasiliauskaite L, Comazzetto S, et al. 2019. A programmed wave of uridylation-primed mRNA degradation is essential for meiotic progression and mammalian spermatogenesis. *Cell Res* **29:** 221–232. doi:10.1038/s41422-018-0128-1

Mullen TE, Marzluff WF. 2008. Degradation of histone mRNA requires oligouridylation followed by decapping and simultaneous degradation of the mRNA both 5′ to 3′ and 3′ to 5′. *Genes Dev* **22:** 50–65. doi:10.1101/gad.1622708

Pandey NB, Marzluff WF. 1987. The stem-loop structure at the 3′ end of histone mRNA is necessary and sufficient for regulation of histone mRNA stability. *Mol Cell Biol* **7:** 4557–4559. doi:10.1128/mcb.7.12.4557-4559.1987

Pirouz M, Du P, Munafo M, Gregory RI. 2016. Dis3l2-mediated decay is a quality control pathway for noncoding RNAs. *Cell Rep* **16:** 1861–1873. doi:10.1016/j.celrep.2016.07.025

Potter-Birriel JM, Gonsalvez GB, Marzluff WF. 2021. A region of SLBP outside the mRNA-processing domain is essential for deposition of histone mRNA into the *Drosophila* egg. *J Cell Sci* **134:** jcs251728. doi:10.1242/jcs.251728

Rissland OS, Norbury CJ. 2009. Decapping is preceded by 3′ uridylation in a novel pathway of bulk mRNA turnover. *Nat Struct Mol Biol* **16:** 616–623. doi:10.1038/nsmb.1601

Sanjana NE, Shalem O, Zhang F. 2014. Improved vectors and genome-wide libraries for CRISPR screening. *Nat Methods* **11:** 783–784. doi:10.1038/nmeth.3047

Seal RL, Denny P, Bruford EA Gribkova AK, Landsman D, Marzluff WF, McAndrews M, Panchenko AR, Shaytan AK, Talbert PB. 2022. A standardised nomenclature for mammalian histone genes. *Epigenetics Chromatin* (in press).

Shalem O, Sanjana NE, Hartenian E, Shi X, Scott DA, Mikkelsen TS, Heckl D, Ebert BL, Root DE, Doench JG, et al. 2014. Genome-scale CRISPR-Cas9 knockout screening in human cells. *Science* **343:** 84–87. doi:10.1126/science.1247005

Slevin MK, Meaux S, Welch JD, Bigler R, Miliani de Marval PL, Su W, Rhoads RE, Prins JF, Marzluff WF. 2014. Deep sequencing shows multiple oligouridylations are required for 3′ to 5′ degradation of histone mRNAs on polyribosomes. *Mol Cell* **53:** 1020–1030. doi:10.1016/j.molcel.2014.02.027

Tan D, Marzluff WF, Dominski Z, Tong L. 2013. Structure of histone mRNA stem-loop, human stem-loop binding protein, and 3′hExo ternary complex. *Science* **339:** 318–321. doi:10.1126/science.1228705

Thomas MP, Liu X, Whangbo J, McCrossan G, Sanborn KB, Basar E, Walch M, Lieberman J. 2015. Apoptosis triggers specific, rapid, and global mRNA decay with 3′ uridylated intermediates degraded by DIS3L2. *Cell Rep* **11:** 1079–1089. doi:10.1016/j.celrep.2015.04.026

Thornton JE, Chang HM, Piskounova E, Gregory RI. 2012. Lin28-mediated control of let-7 microRNA expression by alternative TUTases Zcchc11 (TUT4) and Zcchc6 (TUT7). *RNA* **18:** 1875–1885. doi:10.1261/rna.034538.112

Thornton JE, Du P, Jing L, Sjekloca L, Lin S, Grossi E, Sliz P, Zon LI, Gregory RI. 2014. Selective microRNA uridylation by Zcchc6 (TUT7) and Zcchc11 (TUT4). *Nucleic Acids Res* **42:** 11777–11791. doi:10.1093/nar/gku805

Tuck AC, Rankova A, Arpat AB, Liechti LA, Hess D, Iesmantavicius V, Castelo-Szekely V, Gatfield D, Buhler M. 2020. Mammalian RNA decay pathways are highly specialized and widely linked to translation. *Mol Cell* **77:** 1222–1236.e1213. doi:10.1016/j.molcel.2020.01.007

Warkocki Z, Liudkovska V, Gewartowska O, Mroczek S, Dziembowski A. 2018. Terminal nucleotidyl transferases (TENTs) in mammalian RNA metabolism. *Philos Trans R Soc Lond B Biol Sci* **373:** 20180162. doi:10.1098/rstb.2018.0162

Welch JD, Slevin MK, Tatomer DC, Duronio RJ, Prins JF, Marzluff WF. 2015. EnD-Seq and AppEnD: sequencing 3′ ends to identify nontemplated tails and degradation intermediates. *RNA* **21:** 1375–1389. doi:10.1261/rna.048785.114

Yang XC, Purdy M, Marzluff WF, Dominski Z. 2006. Characterization of 3′hExo, a 3′ exonuclease specifically interacting with the 3′ end of histone mRNA. *J Biol Chem* **281:** 30447–30454. doi:10.1074/jbc.M602947200

Zuber H, Scheer H, Ferrier E, Sement FM, Mercier P, Stupfler B, Gagliardi D. 2016. Uridylation and PABP cooperate to repair mRNA deadenylated ends in *Arabidopsis*. *Cell Rep* **14:** 2707–2717. doi:10.1016/j.celrep.2016.02.060

See the following page for ***Meet the First Authors***

MEET THE FIRST AUTHORS

Chris Holmquist

Wenxia He

***Meet the First Author(s)* is a new editorial feature within *RNA*, in which the first author(s) of research-based papers in each issue have the opportunity to introduce themselves and their work to readers of *RNA* and the RNA research community. Chris Holmquist and Wenxia He are the co-first authors of this paper, "Knockouts of TUT7 and 3′hExo show that they cooperate in histone mRNA maintenance and degradation." Chris did this work while he was a graduate student in Bill Marzluff's lab at UNC Chapel Hill, as a major part of his dissertation. Wenxia is a postdoctoral fellow in the Bill Marzluff's laboratory, with a research interest in the multiple mechanisms that control histone gene expression, focusing on the biochemical details of histone mRNA degradation.**

What are the major results described in your paper and how do they impact this branch of the field?

Rapid histone mRNA degradation is an important regulatory mechanism in coordinating histone protein synthesis and DNA replication during S-phase. Here, using CRISPR technology, we describe the role of a specific uridyl terminal transferase, TUT7 (TENT3B, ZCCHC11), and a specific 3′ to 5′ exonuclease, 3′hExo (Eri1), in both maintaining active histone mRNA during S-phase and in rapidly degrading histone mRNA when DNA replication is inhibited in S-phase or completed at the end of S-phase. While TUT7 and TUT4 are involved in degradation of many RNAs, this is the first example of a specific role for TUT7 that can't be carried out by TUT4, in degradation of a specific set of mRNAs.

What led you to study RNA or this aspect of RNA science?

CH: I started out interested in pharmaceutical development, and in particular novel strategies away from small molecule screens. This led me toward RNA aptamers, and after taking a course on RNA with Bill Marzluff, I was hooked on the mechanism of how they were regulated! Every time I learned more about how RNA is regulated or utilized in the cell, it brought up more questions and new functions. Bill provided me a place to study and investigate histone mRNA while using CRISPR and deep sequencing as it was exploding in the research scene.

WH: I studied SLBP in zebrafish as a PhD student, and described two different SLBPs that function to regulate histone mRNA and protein synthesis in zebrafish embryogenesis, which was published in *RNA*. One of the zebrafish SLBPs is the ortholog of mammalian SLBP, and histone mRNA is its only known target RNA. This brought me to apply to and join Bill Marzluff's lab, which has carried out nearly half a century of research on histone mRNA expression and regulation.

What are some of the landmark moments that provoked your interest in science or your development as a scientist?

CH: While in high school, I had a phenomenal chemistry teacher, Ms. Ugalde, who showed me that the molecular world is a complex system built on rules, some known and unknown. From there, my undergraduate professor Dr. Kundalkar continued to encourage me to pursue biology questions using chemistry, which led me to medicinal chemistry. Bill Marzluff is the one who shined the light on genetics and helped me realize that RNA is so much more than the central dogma, and is an enigma that I could study forever! He also showed a lot of patience while I learned new molecular systems to study RNA, which was key to my development as a scientist.

WH: As a graduate student, the lab I was in had identified SLBP2 in a genetic screen in carp. I used the powerful zebrafish system to determine the function of this gene in zebrafish. This taught me the power of genetics, and I am now studying both biochemical mechanisms in mammalian cells and genetics in *Drosophila*, to better understand the complex regulation of histone mRNA; using CRISPR in both systems, I now realize the importance of developing multiple approaches to solve a complex problem. It's so important to know the whole picture and the background of the problem you are studying, and to be willing to use multiple approaches and different systems to best solve biological problems.

Are there specific individuals or groups who have influenced your philosophy or approach to science?

CH: First and foremost, my advisor Bill Marzluff. He showed me that diversity in background, both scientific and personal, improves the scientific process. Different philosophies and cognitive styles bring new ideas and approaches. My undergraduate professor Dr. Kundalkar and high school teacher Ms. Ugalde both taught me that kindness is essential when we face so many negative results. Rita and Michelle both helped me look at my project with new eyes, and come up with solutions I never could have if I was isolated. We all taught and learned from each other, equally. Finally, my wife, Chelsea Raulerson. She was also my computational biologist and helped me reevaluate my approach to data analysis and how I represent my results, along with an appreciation for computational biology's growing role in the world of RNA.

WH: First, my mentor, Bill, is amazing and has helped me a lot. He is always ready to provide any support he can and is very good at figuring out the best experiments to do in a short amount of time. The other labs around us have been particularly helpful. In addition to Rita who was an expert on lentivirus, the members of Alain Laederach's lab, particularly Leila, always helped me with interpreting the sequencing, and the student Nicole in Jill Dowen's

Continued

lab taught me how to use the CRISPR screening technology, both for designing experiments and screening the cells. I have learned Drosophila genetics from Bob Duronio's lab, particularly from Jim Kemp in that lab, which has been essential in my other work.

What are your subsequent near- or long-term career plans?

CH: While I enjoyed doing the bench work, I found I had a passion and skill for professional development. Currently, I work as an academic advisor for undergraduate biologists, and hope to continue to help early career scientists develop skills and strategies to improve not just their research but discover how their skills as scientists can be used in their future careers!

WH: I really hope to figure out the whole complex for histone mRNA degradation in the next few years, and am currently collaborating with a group in Germany. It is one of the most important parts for histone mRNA regulation and is a novel pathway different from degradation of most mRNAs. In the long term I would like to have my own independent research program.

What were the strongest aspects of your collaboration as co-first authors?

CH: Wenxia came in and gave me peace of mind that this project would be in great hands. I had spent a long time creating these knockouts and optimizing the deep sequencing to determine their phenotypes; but the question of the rescue experiments was out of my grasp. Wenxia came in and was able to successfully rescue quite a large protein and complete the story with a very satisfying conclusion! No one likes a story that isn't finished. I was about to graduate and move before things grinded to a halt, and Wenxia joined the lab and offered to help finish the story. While we overlapped briefly, she picked up where I was leaving off with such ease! Within weeks I knew that she would find a conclusion to the story, and continue to explore the exciting world of histone mRNA regulation.

WH: Since Chris was close to graduation (and the pandemic had started making it difficult to continue work for a while), completion of the project was substantially delayed. Chris had created the CRISPR mutants and done much of the analysis when I joined the lab. I took charge of designing and cloning the rescue vectors, since multiple approaches had failed. Successful completion of the rescue experiments was important for the finishing the entire story.